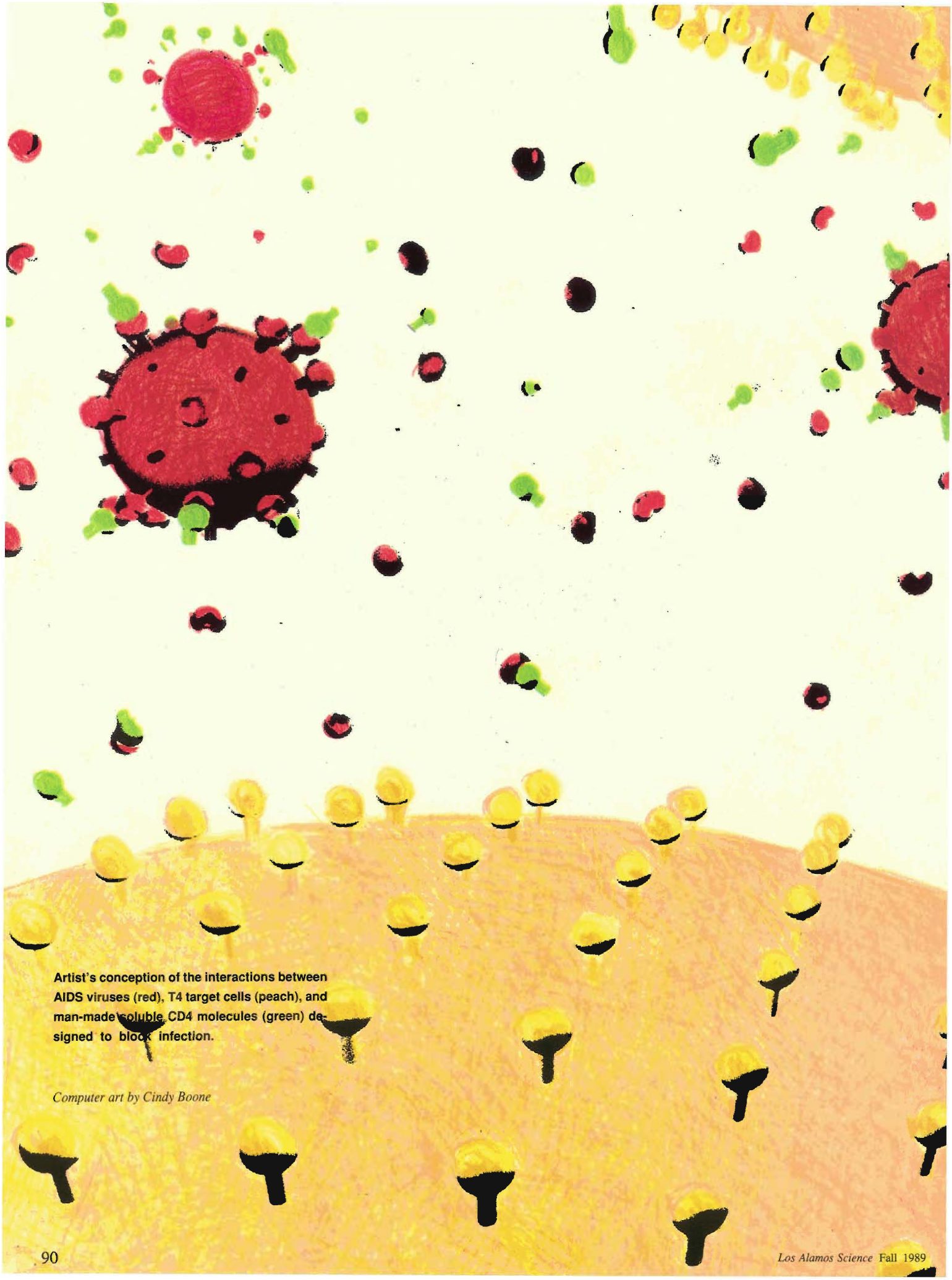

Artist's conception of the interactions between AIDS viruses (red), T4 target cells (peach), and man-made soluble CD4 molecules (green) designed to block infection.

Computer art by Cindy Boone

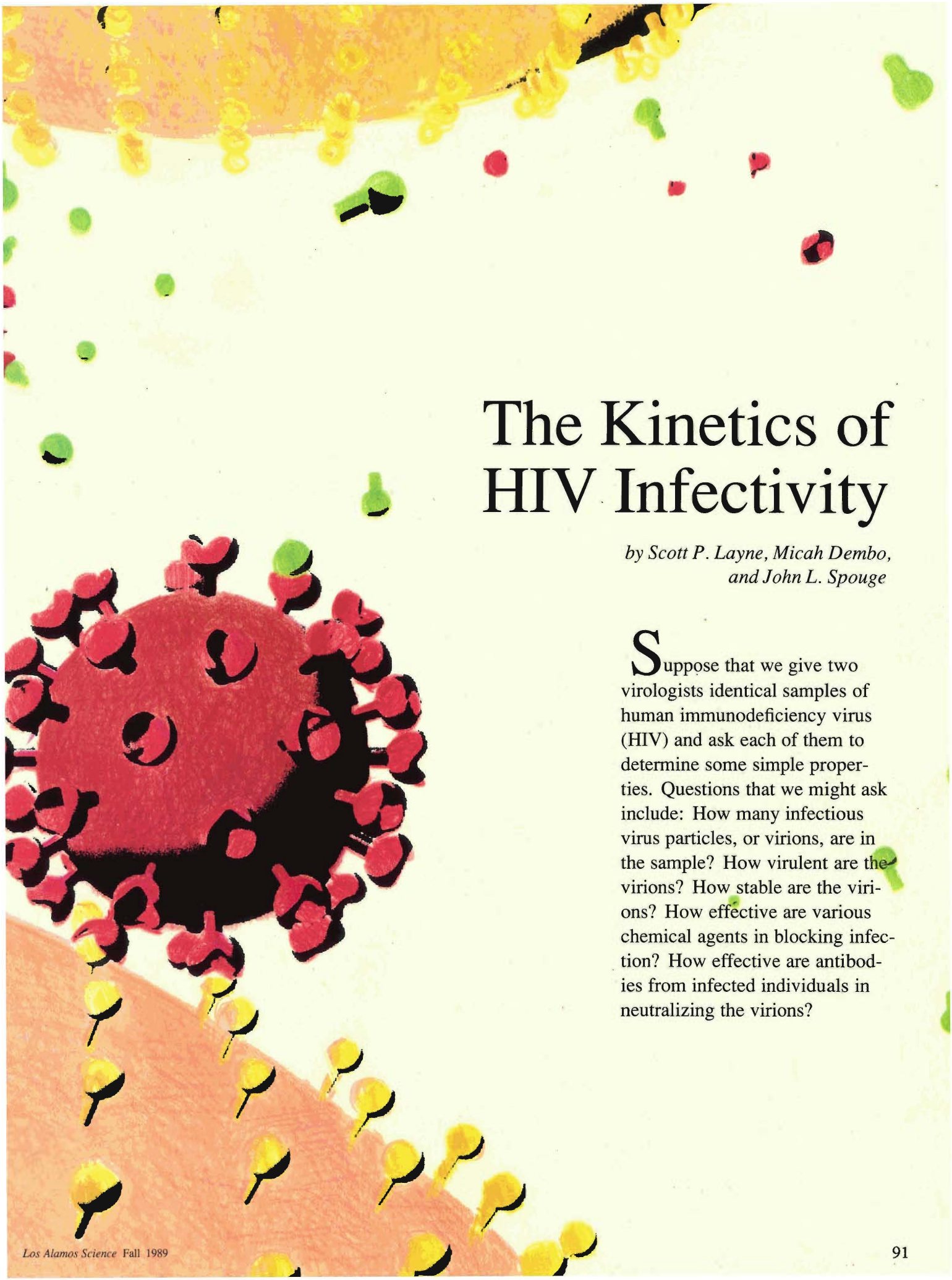

The Kinetics of HIV Infectivity

by Scott P. Layne, Micah Dembo, and John L. Spouge

Suppose that we give two virologists identical samples of human immunodeficiency virus (HIV) and ask each of them to determine some simple properties. Questions that we might ask include: How many infectious virus particles, or virions, are in the sample? How virulent are the virions? How stable are the virions? How effective are various chemical agents in blocking infection? How effective are antibodies from infected individuals in neutralizing the virions?

The virologists would set about answering our questions by running a series of viral infectivity assays, in which specific conditions would be tailored to tackle each particular problem (Fig. 1). For example, to deal with the question of blocking agents, the virologists would inoculate aliquots of our sample virus into a series of chambers, each containing target cells plus a different concentration of blocker. The effectiveness of the blocker could be judged by the amount required to reduce target-cell infection by one-half relative to an untreated control. Despite the superficial appearance of scientific rigor, it would not be surprising to find that the two virologists (with the best of intentions and technique) obtained significantly different results for the same blocking agent and viral strain. With further inquiry we would most likely discover that the virologists used somewhat different assay conditions, that is, different target-cell types, cell concentrations, viral-inoculation techniques, and so on. To understand the underlying causes of the discrepancy, we would need to integrate a great deal of detailed and quantitative information. Only then could we judge which result might be most representative of the agent's activity in clinical situations.

The difficulty of comparing the results of one assay method with those of another is one of the biggest headaches in virology. That problem is particularly important in the case of HIV because the screening for potential therapeutic agents and vaccines against HIV is frequently based on assay results alone. To improve the utility of such assays, it is useful to study theoretical models of the kinetic processes that determine their outcomes.

In this article we present a model for the kinetics of HIV infection in assay systems. We show how to use the model for designing and analyzing viral infectivity assays and for answering the kinds of questions posed above. We also use the model to evaluate prospects for blocking therapies and vaccines.

Elements of a Viral Infectivity Assay

HIV infects subsets of lymphocytes, monocytes, and macrophages exhibiting the CD4 protein on their surfaces. Such $CD4^+$ cells manifest infection through a spectrum of outcomes ranging from prolonged latency to cell fusion and cell death. Sometimes replication is so explosive that target cell membranes lyse as newborn virions emerge. Unfortunately, $CD4^+$ cells are at the helm of the immune system's response to microbial invasion. Thus HIV infection not only harms individual target cells but also perturbs the entire communication network for the body's defenses. The result is a catastrophic susceptibility to opportunistic infections. (For more details see "AIDS Viruses in Animals and Man: Nonliving Parasites of the Immune System.")

Viral infectivity assays involve great kinetic complexity, but they are still much simpler than the infective process in vivo. For example, in assays only a single type of target cell is present and only the primary infections caused by the initial virions added to the assay chamber are studied (Fig. 1). In vivo, direct cell-to-cell transmission of infection and the prolonged growth and reproduction of the virus come into play. Assays also neglect the effects of the normal immune responses blocking infection; clearly these are extremely important in vivo.

To formulate a model of an assay system, lets start by considering an ideal-

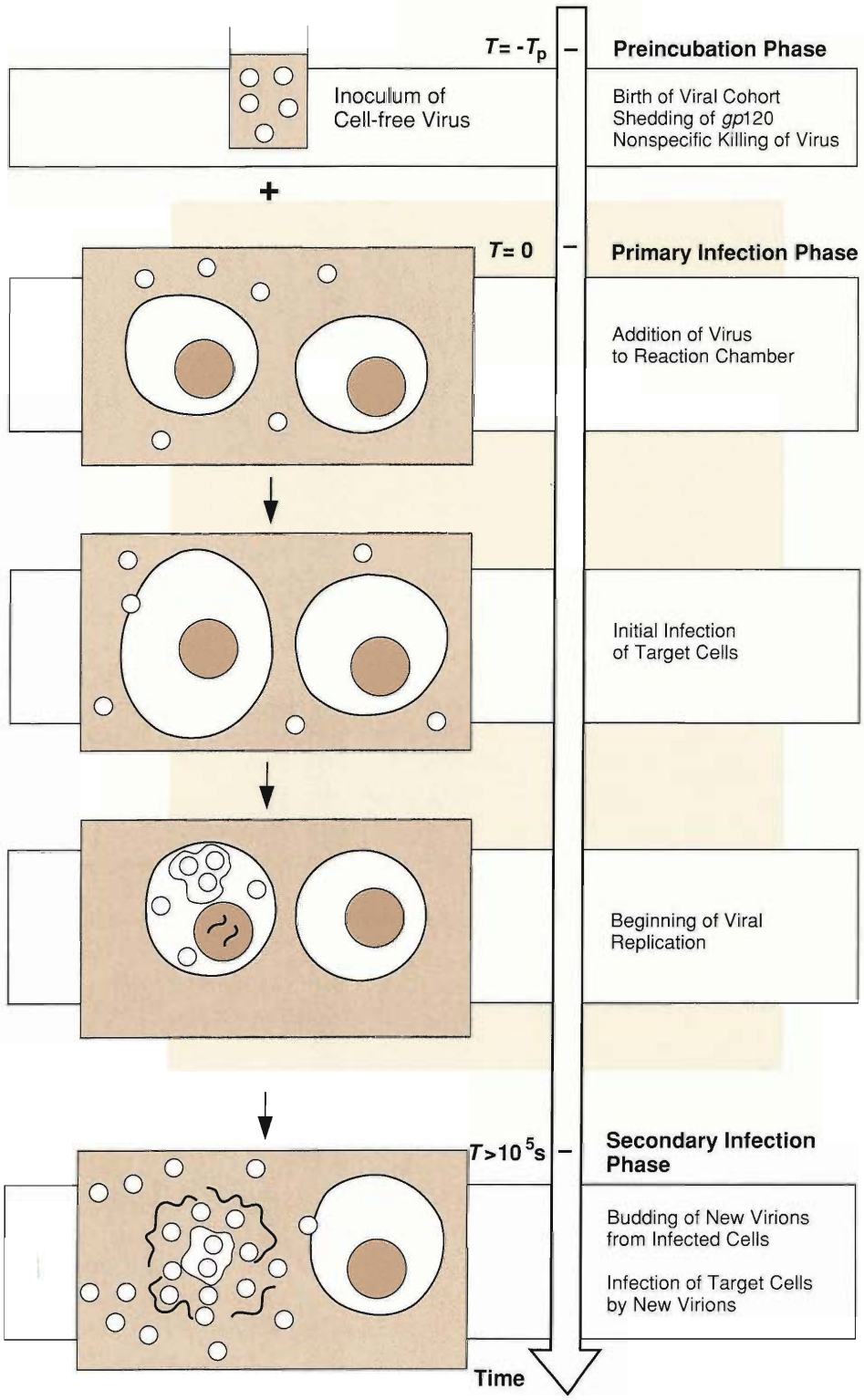

PHASES IN A VIRAL INFECTIVITY ASSAY

Fig. 1. Schematic diagram of the three phases of a viral infectivity assay. The inoculum is prepared by growing HIV in cell cultures and centrifuging the supernatant to separate virions from cellular debris and is then stored for a "pre-incubation" time T_p. For simplicity we assume that the inoculum consists of a "homogenous cohort" of virions born at $T = -T_p$. During the pre-incubation phase, $-T_p \leq T \leq 0$, the virions become less infectious as they shed *gp*120 and can also be killed by nonspecific agents, but target-cell infection does not occur. To begin the primary infection phase, a calibrated number of virions is added to the target cells in the reaction chamber at $T = 0$. During the primary infection phase, $0 \leq T \leq 10^5$ seconds, *gp*120 shedding, nonspecific killing, and target-cell infection occur. Ordinarily HIV replicates within 24–48 hours ($\sim 10^5$ seconds) after entering a target cell. During the secondary infection phase, $T > 10^5$ seconds, new virions emerge from cells infected during the primary infection phase and secondary infections occur. The secondarily infected cells then produce new virions, which infect other cells, and so on. A viral infectivity assay is said to be linear if the additional cycles of infection produce virions (or viral proteins) in proportion to the number of initial infections.

RELATING THEORY TO EXPERIMENT

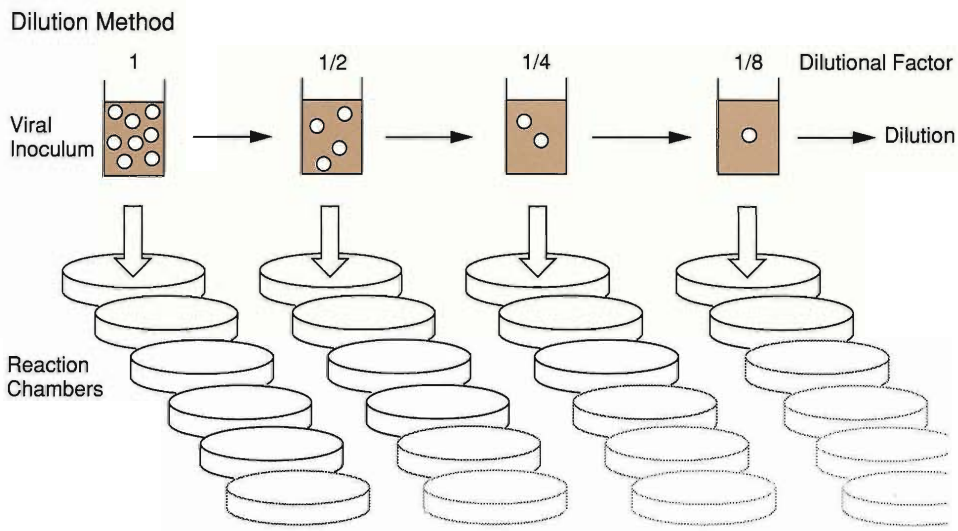

Fig. 2. Most experimental assays determine *I*, the number of cells produced during the primary infection phase (see Fig. 1) by a dilution method known as the ID-50 method. As shown on the diagram, a viral stock solution is inoculated into a large number of assay chambers (usually 10 to 20) and the infection is allowed to go to completion. The experiment is then repeated again and again, each time with a more dilute solution, until no infections occur in half the chambers. The reciprocal of the dilution factor required to achieve this result is called ID-50 (infectious dose—50 per cent). Now, when half the chambers have no infection, we can say that the probability of the diluted viral stock solution's infecting 0 cells is 0.5, or $p_0 = 0.5$. But since the probability of a viral stock solution's infecting k cells is described by a Poisson distribution, that is, since $p_k = e^{-I}/I^k k!$, then $p_0 = e^{-I}$ or $I = \ln p_0$. Thus $I_{\text{diluted}} = \ln 2$. We determine I for the original stock solution by multiplying ln 2 by ID-50. Having determined I, it can be used to obtain an estimate of V_0. Since $i \equiv I/V_o$, if the assay is performed under conditions such that $i \approx 1$ ($T_p \to 0$ and $L \to \infty$), then $V_0 \approx I$.

ized solution containing a "homogeneous cohort" of free virions of a particular HIV strain. A homogeneous cohort is defined as a population of virions that were born simultaneously and that have been treated identically ever since. (An actual stock solution of virus will consist of a mixture of homogeneous cohorts but it is simplest to treat each cohort separately. This involves no loss of generality, since we can readily obtain all the properties of a mixture of cohorts by taking a weighted average.) We can imagine that the members of the homogeneous cohort were born at some time in the past $T = -T_p$.

At $T = 0$, we inoculate V_0 random members of the viral cohort into a chamber containing a much larger number of $CD4^+$ target cells. At some later time $T > 0$, some of these will have successfully infected target cells. That number, call it $I(T)$, is the primary quantity of biological interest. $I(T)$ is related to the probability that a single virion will successfully infect a target cell by time T; that is, $i \equiv I/V_0$,. It is worth mentioning that if we keep the size of our inoculum sufficently small relative to the number of target cells then the number of successfully infecting virions will be equal to the number of infected cells. Figure 2 describes how I is actually measured experimentally.

Once an assay is underway, a number of kinetic processes occur simultaneously. Infection of target cells occurs in multiple stages: first, a virus diffuses to the cell surface; second, the *gp*120 glycoproteins on the virus's surface and CD4 on the target cell's surface form bimolecular complexes; and third, interactions involving CD4, *gp*120, and *gp*41 (which is attached to *gp*120) promote fusion of the HIV envelope with the target-cell membrane, resulting in entry of the viral core into the cell. Subsequently reverse transcription of the viral genome, its incorporation into the genome of the host, and production of new virions complete the life cycle. Before they penetrate target cells, the virions in the assay chamber are subject to several degrada-

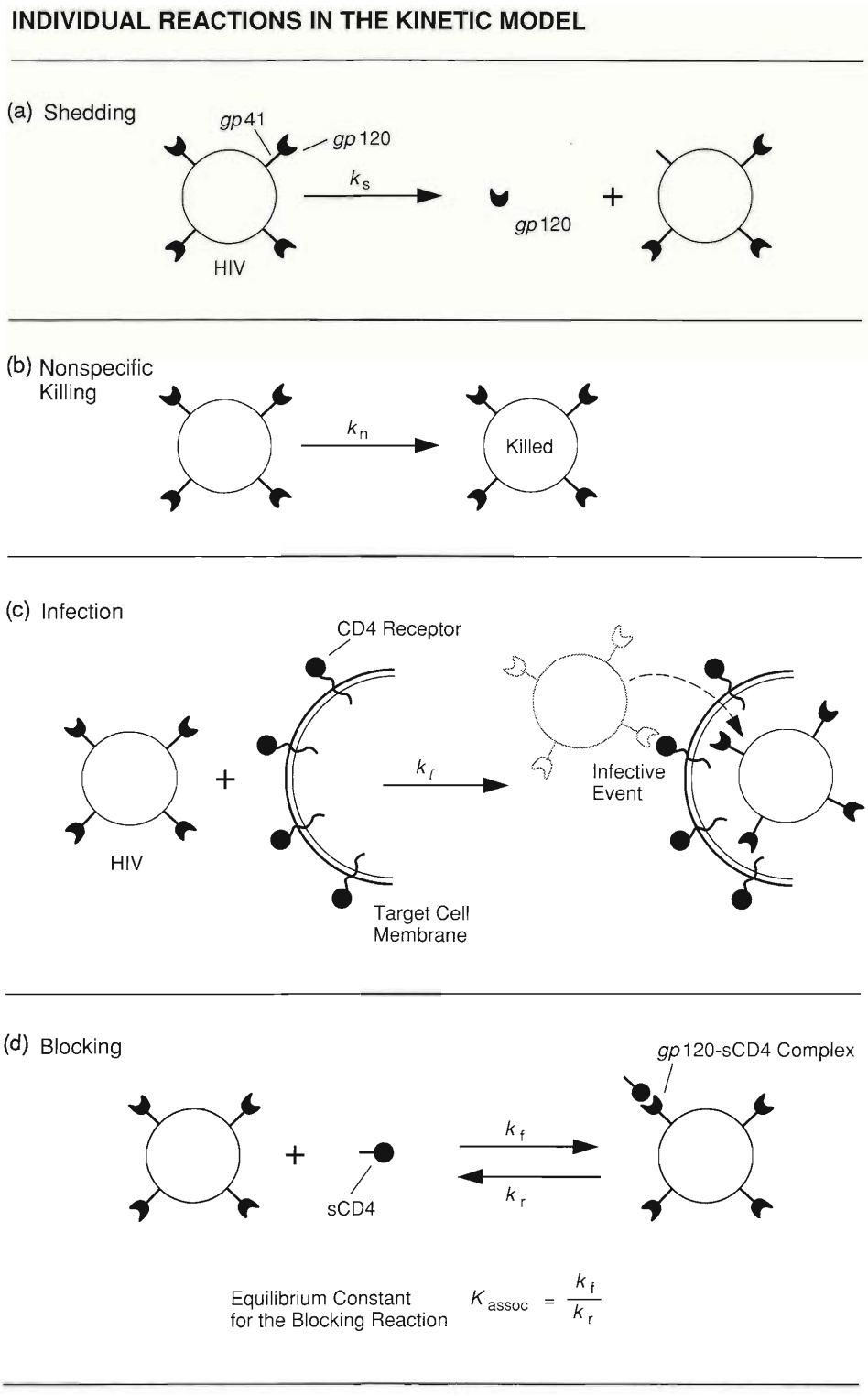

Fig. 3. Schematic diagram of the kinetic processes in a viral infectivity assay. The level of detail shown here mirrors the treatment in our kinetic model. (a) The process that complicates the kinetics of the model is the spontaneous shedding of *gp*120 from so-called live virions; that is, *gp*120 spontaneously dissociates from *gp*41. The rate constant for shedding of *gp*120 is k_s. Once a *gp*120 molecule is shed, it cannot bind again to a virion so we do not keep track of it in our kinetic model. The irreversible shedding process causes progressive inactivation of virions; that is, the virions become less and less infectious. When they lose all of their *gp*120s, they are inactive but still subject to nonspecific killing mechanisms, shown schematically in (b). Nonspecific killing mechanisms include enzymatic degradation and dissolution by soaps such as nonoxynol-9, a component of common spermicides. In (c) we show an infective event, that is, the entry of a virion into a target cell where it can begin to replicate. We do not model that process in detail but rather assume the total rate of infection in the assay chamber is proportional to $k_\ell F$, where F is the number of *gp*120s attached to living virions and k_ℓ is a rate constant that combines all quantities involved in collision of a virion and a target cell, binding of *gp*120 to CD4, fusing of the virion with the cell membrane, entry of the viral core, and integration of the viral genome into the genome of the target cell. We assume k_ℓ remains constant during the assay, whereas F is continuously changing. In (d) we show the reversible blocking reaction between soluble CD4 (sCD4) and the *gp*120 molecules on the surface of a live virion. The parameters k_f and k_r are the forward and reverse rate constants, respectively, for the complexing of *gp*120 with sCD4 (that is, for the formation and dissociation of *gp*120-sCD4 complexes). Those processes result in the masking and unmasking of *gp*120s but do not result in a net loss of *gp*120 from the reaction chamber nor in the disappearance of live virions.

TIME DEPENDENT KINETICS

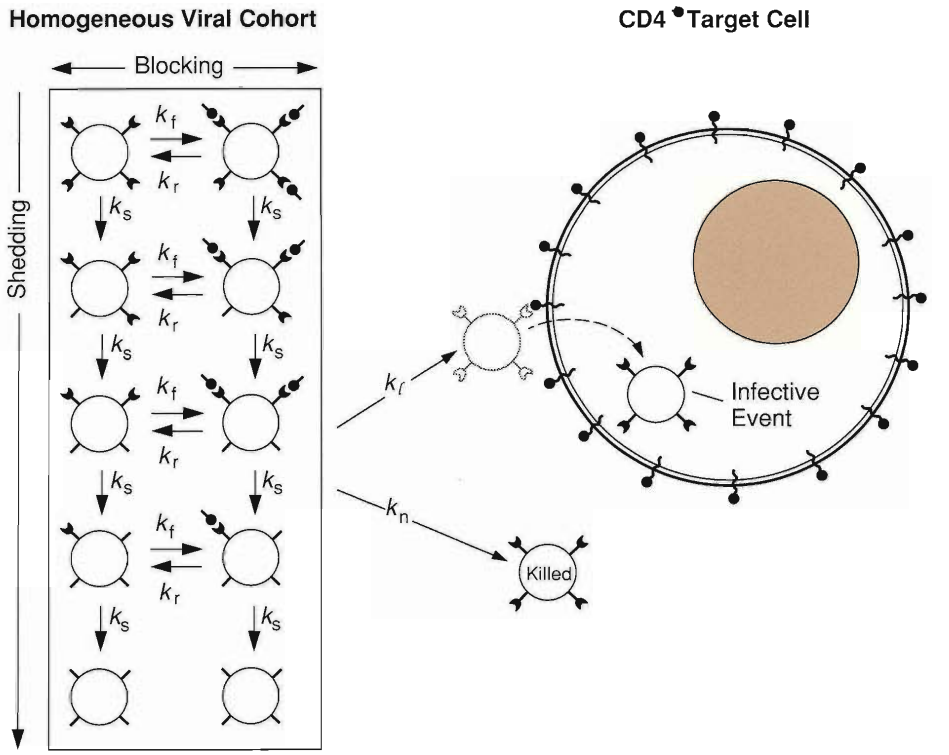

Fig. 4. All processes shown in Fig. 3 occur simultaneously during the primary infection phase of a viral infectivity assay. Notice that a virion may exist in one of many different states at the time it encounters a target cell. A live virion that has lost all its *gp* 120s cannot infect target cells and is therefore inactive. As time progresses, the live virions continually shed *gp*120 from their surfaces. Also, the blocker sCD4 may bind to and then dissociate from the free *gp*120s on the virion surfaces. The rate of infection of target cells is assumed to be proportional to $k_f F$. We assume that an infective event causes the loss from the medium of the infecting virion along with the free *gp*120s and *gp*120-sCD4 complexes on its surface.

tive processes that alter their ability to complete a life cycle: most important, HIV spontaneously sheds, over a period of hours, the seventy to eighty *gp*120 molecules present on its surface at birth. After shedding all its *gp*120s, a virion can no longer bind to a target cell. HIV may also be under attack by antibody, by enzymes naturally present in the surrounding medium, or by other viracidal agents added to the assay chamber. Neutralization, degradation, and dissolution of the virions by such agents is usually irreversible and will be referred to as nonspecific killing. Finally, the infectiousness of virions may be reversibly inhibited by a blocking agent (for example, soluble CD4, abbreviated sCD4) that forms a complex with *gp*120 and thereby prevents it from binding to target cells. Figure 3 illustrates schematically the rate laws that we propose govern the kinetic processes described above. Figure 4 illustrates how the processes are integrated to give a closed system of equations. We should emphasize that, although these rate laws are plausible, definitive tests are not yet available.

The Rate Equations

The rate equations are formulated in terms of four dependent variables $F,C,V,$ and I. These represent, respectively, the number of free *gp*120 molecules present

on living virions in the assay chamber, the number of complexed *gp*120 molecules present on living virions in the assay chamber, the number of living viral particles in the chamber, and the number of infected cells in the chamber. There are also several independent variables; these are: time T, the preincubation time T_p, the concentration B of the blocking agent sCD4, the size of the inoculum V_0, and the concentration of target cells L. Finally, there are constant parameters: the initial number of *gp*120 molecules on each virion at birth N and the five rate constants k_ℓ, k_n, k_s, k_f, and k_r defined in Fig. 3. In terms of these quantities the rate equations are:
Rate of Target-Cell Infection:

$$\frac{dI}{dT} = k_\ell LF . \tag{1}$$

Rate of Loss of Live Virions:

$$\frac{dV}{dT} = -k_\ell LF - k_n V . \tag{2}$$

Rate of Change of Number of Free *gp*120s:

$$\frac{dF}{dT} = -k_f BF + k_r C - (k_s + k_n)F - k_\ell LF \left[1 + (N - 1)\frac{F}{NV}\right] . \tag{3}$$

Rate of Change of *gp*120-sCD4 Complexes:

$$\frac{dC}{dT} = k_f BF - k_r C - (k_s + k_n)C - k_\ell LF \left[(N - 1)\frac{C}{NV}\right] . \tag{4}$$

The term $k_\ell LF$ on the right of Eq. 1 represents the total rate of target-cell infection in the assay chamber. This rate law incorporates the notion that infection requires the combination of a free *gp*120 molecule with a target cell. Moreover, this rate law assumes that in some sense all *gp*120s are equivalent in their potential to initiate an infection. One corollary of this assumption of equivalence is that an individual virus particle must infect at a rate proportional to the number of free *gp*120s on its surface.

The term $k_n V$ on the right of Eq. 2 represents the rate of loss of live virions due to nonspecific killing. Note that virions are also lost at a rate $k_\ell LF$, due to penetration of target cells.

The terms $k_f BF$ and $k_r C$ on the right of Eqs. 3 and 4 are the rates of formation and dissociation of *gp*120-sCD4 complexes, respectively. The terms $(k_s + k_n)F$ and $(k_s + k_n)C$ are the rates of loss of free and complexed *gp*120, respectively, due to the combined effects of spontaneous shedding and nonspecific killing. These rate laws imply that when a virus is nonspecifically "killed" there is concomitant loss of all the free and complexed, *gp*120s on its surface. As far as our theory is concerned, these completely disappear from the system and have no further kinetic role. In a similar way, shedding of a free or complexed *gp*120 molecule is equivalent to loss of this molecule from the system. It is also apparent that for these rate laws to hold exactly,

the processes of nonspecific killing and shedding must operate equally on all the free and complexed $gp120$ molecules in the system.

Finally, the terms $k_\ell LF[1 + (N - 1)F/NV]$ and $k_\ell LF[(N - 1)C/NV]$ are the rates of loss of free and complexed $gp120$ molecules due to infective events. Once again these terms hold rigorously only if each free $gp120$ remaining in the system has an equal chance of initiating an infective event. The proof proceeds from the fact that only one free $gp120$ is required to initiate an infective event. There will also be some additional $gp120$s that disappear (are internalized) as a byproduct of an infective event. By calculating the appropriate conditional expectations, one can show that the average number of such losses per event will be $(N-1)F/NV$ free and $(N-1)C/NV$ complexed $gp120$ molecules.

To uniquely solve the rate equations, we must specify the conditions at the start of the primary infection phase ($T = 0$). To do this in a simple way, let's suppose that before the virions are added to the assay chamber, they are isolated from target cells and blocker. Therefore, L, B, I, and C are all equal to zero between $T = -T_p$ and $T = 0$. Solving Eqs. 2–5 we easily find that the initial conditions at $T = 0$ are : $I = 0$, $V = V_0 \exp\left(-k_n T_p\right)$, $F = NV_0 \exp\left[-(k_n + k_s)T_p\right]$, and $C = 0$.

Parameter Estimation

By proposing our model we have, at least in principal, reduced the problem of physically characterizing the kinetics of viral infection to the problem of determining N and the five rate constants k_ℓ, k_f, k_r, k_s, and k_n. Unfortunately, satisfactory experimental measurements of these parameters are not yet available. Thus the problem of designing experiments for determining parameters is one of the major goals of our analysis (see following section on determining rate constants). For the present we will simply indicate how one may derive some rough a priori estimates of the parameters. These will be useful for generating illustrative numerical solutions (see following section).

The rate constant for target cell infection k_ℓ, is an overall rate constant for the multiple stages involved in the infection of a target cell by a virion (that is, its binding to an sCD4 receptor, its fusing with the cell, and so on). It should be remembered however that the rate constant is defined on a "per free $gp120$" basis and not on a "per virus" basis. From this definition it can easily be seen that the upper limit of k_ℓ must occur when every diffusive encounter between a free $gp120$ molecule attached to a viron and a target cell results in infection. After taking into account the diffusion constants of a virion and of a target cell and after correcting for the fraction of the virion's surface that is covered by a single $gp120$, the diffusion-limited approximation yields a value for k_ℓ of about 8×10^{-13} cm^3 s^{-1}.

Similarly, the diffusion-limited approximation for the rate constant for collision between sCD4 and $gp120$ yields an upper limit for the forward rate constant for blocking: $k_f \leq 3 \times 10^{-12}$ cm^3 s^{-1}.

To estimate a value for k_r, the reverse rate constant for blocking, we use the results of equilibrium-binding experiments. Those tell us that K_{assoc}, the equilibrium constant for association between sCD4 and $gp120$ is about 2.0×10^{-12} cm^3 per molecule. Then, since $K_{assoc} \equiv k_f/k_r$, we estimate that $k_r = k_f/K_{assoc} \leq 1.5$ s^{-1}.

Electron-microscope studies on the structure of HIV indicate that seventy to eighty *gp*120 molecules completely cover the surface of a mature virion. Therefore, we take $N = 80$.

Finally, to estimate the rate constant for nonspecific killing k_n and the rate constant for shedding of *gp*120 from a live virion k_s, we use Peter Nara's results for two strains of the human T-lymphotropic virus III. He showed that those strains lose half of their infective activity within 4 to 6 hours when incubated in their growth media at 37°C. That implies that both k_s and k_n are less then about 10^{-4} s^{-1}.

Numerical Solutions

Having specified the inital conditions and obtained estimates for the rate constants, we can solve the rate equations numerically. The sample solutions shown in Fig. 5 help us gain insight into the temporal behavior of the model. The average numbers of live virions, infected target cells, and free *gp*120's and *gp*120-sCD4 complexes on the surface of live virions are desplayed as nondimensional variables (see "Mathematical Considerations" for definitions). Figure 5a shows a case with no blocker ($B = 0$); Fig. 5b and Fig. 5c show the effect of adding a low and a higher concentration of blocker; Fig. 5d shows the effects of a high concentration of blocker in conjunction with a nonspecific killing agent (for example, nonoxynol-9).

When no blocker is present (Fig. 5a), the number of infected target cells rises linearly until $T \approx 10^3$ seconds. Subsequently, at the characteristic shedding time ($k_s^{-1} \approx 10^4$ seconds), the number of free *gp*120 molecules drops, and the rate of target-cell infection diminishes. The obvious decline in the number of live virions at $T \approx 10^3$ seconds is due to target-cell infection. When target-cell infection stops at $T \approx 10^5$ seconds, 72 per cent of the initial number of live virions have infected target cells; the remaining 28 per cent, now completely lacking *gp*120 molecules and hence inactive or noninfectious, remain in the medium. Since nonspecific killing was not included in this computation, the inactive live viral particles remain in solution indefinitely.

Figure 5b shows the effects of adding a low concentration of the blocking agent sCD4 to the culture medium. The presence of sCD4 does not affect the rate of target-cell infection until *gp*120 and sCD4 begin to equilibrate at $T \approx 10^{-1}$ second.

After that time the rate of target-cell infection declines by a factor of 2 to 3, and ultimately, only 35 per cent of the live virions infect target cells. The decline compared to case (a), 35/72, is approximately the proportion of *gp*120s blocked by sCD4.

Figure 5c shows the effects of a hundredfold higher concentration of sCD4. Equilibration between the blocker and *gp*120 occurs more rapidly, in only 3×10^{-3} second, and 199 out of every 200 *gp*120 molecules are blocked. The percentage of live virions that infect target cells declines from 72 per cent in case (a) to only 0.36 per cent.

Figure 5d shows the synergy of sCD4 and a nonspecific killing agent. We assign a rate constant for nonspecific killing, $k_n = 5 \times 10^{-4}$ s^{-1}, that is fivefold greater than the rate constant assumed for *gp*120 shedding, $k_s = 10^{-4}$ s^{-1}. As in Fig. 4c, binding of sCD4 to viral *gp*120 and shedding of viral *gp*120 are assumed to be independent

TIME DEPENDENT SOLUTIONS OF THE KINETIC MODEL

Fig. 5. Four numerical solutions of the model illustrating the progress of an untreated infection, an infection treated with two concentrations of sCD4, and an infection treated with sCD4 plus nonspecific killing agent. The corresponding parameters are (a) $B = 0$ and $k_n = 0$, (b) $B = 10^{12}$ molecules cm^{-3} and $k_n = 0$, (c) $B = 10^{14}$ molecules cm^{-3} and $k_n = 0$, and (d) $B = 10^{14}$ molecules cm^{-3} and $k_n = 5 \times 10^{-4}$ s^{-1}. The results are plotted in non-dimensional variables: "Infected Cells" labels a plot of $i \equiv I/V_0$, "Virions" labels a plot of $v \equiv V/V_0$, "Free *gp*120s" labels a plot of $f \equiv F/NV$, and "*gp*120-sCD4 Complexes" labels a plot of $c \equiv C/NV$. For all cases $T_p = 0$ and $L = 2 \times 10^6$ cells cm^{-3}, which is a typical lymphocyte concentration for infectivity assays.

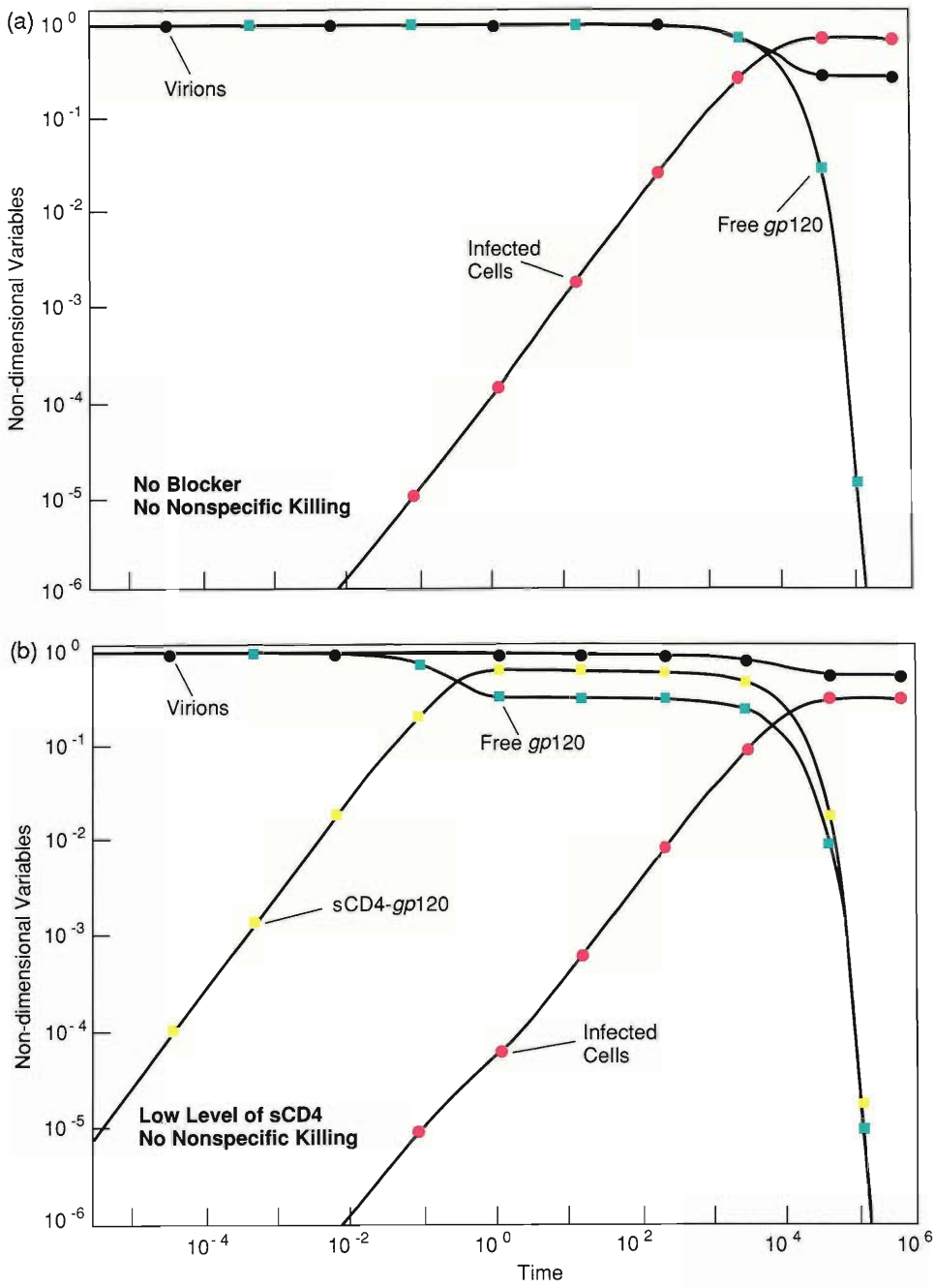

of nonspecific killing, which occurs on a "per live virion" basis. Nonspecific killing causes the disappearance of virions and so infection stops before virions shed all of their *gp*120 molecules. As a result, the ultimate number of infective events per virion is sixfold less than the case shown in Fig. 5c.

Although the time development of infection is of interest, it is usually not possible to freeze the infective process at an intermediate stage. Thus, most experiments

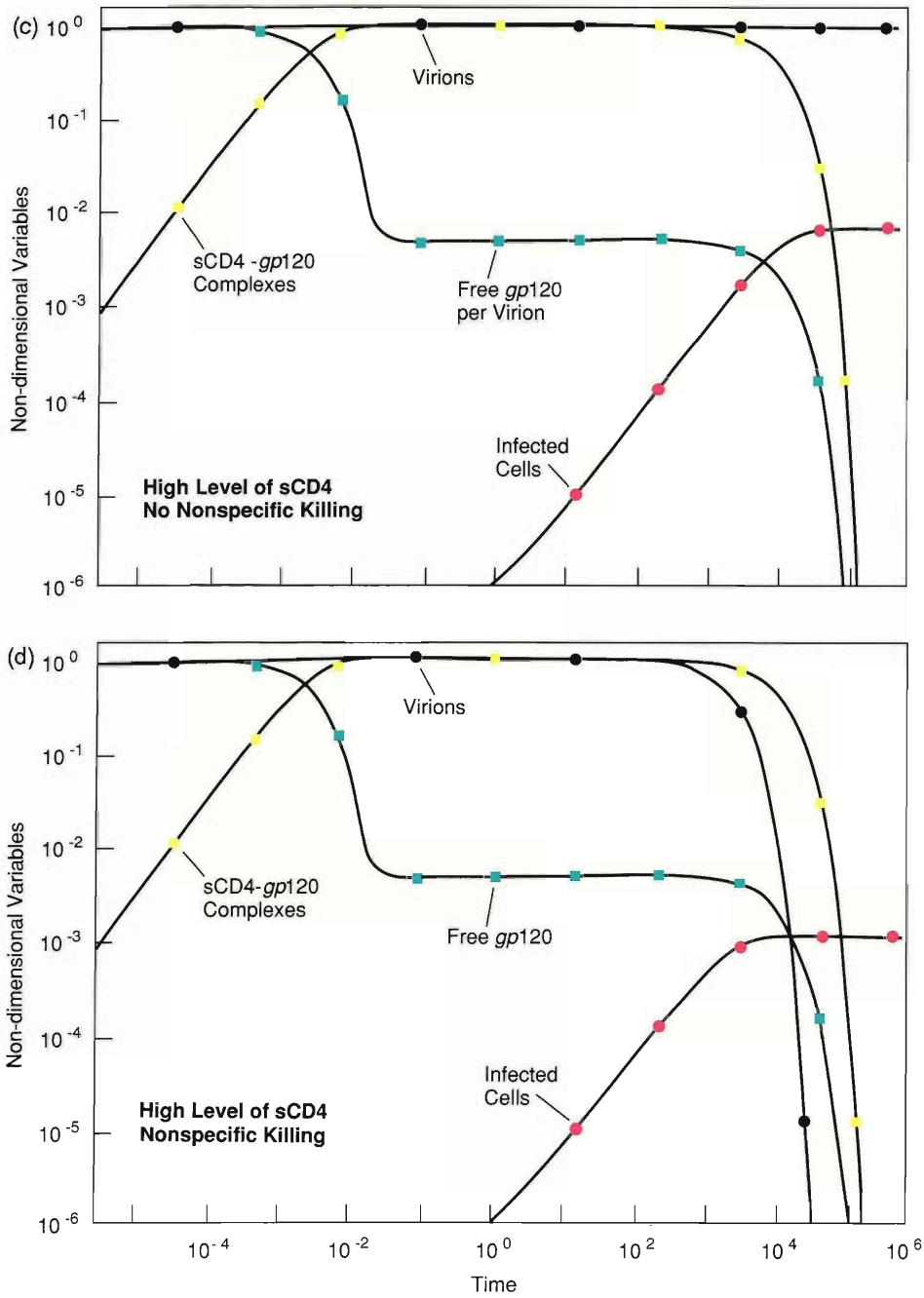

report only the values of $I(T)$ at the end of the primary infection phase (Fig. 1). This quantity is denoted by I_∞. The main theoretical results concerning I_∞ are Eqs. $7', 8'$, and $9'$ of "Mathematical Considerations." Those equations express I_∞ in terms of the nondimensional parameter ζ. From an intuitive point of view ζ is simply a scalar measure of the degree to which the assay conditions favor infection. When $\zeta \to 0$ (for example, when $B \to \infty$ or $L \to 0$), infection is inhibited and I_∞ is approximated

NONLINEAR EFFECTS OF TARGET-CELL CONCENTRATION

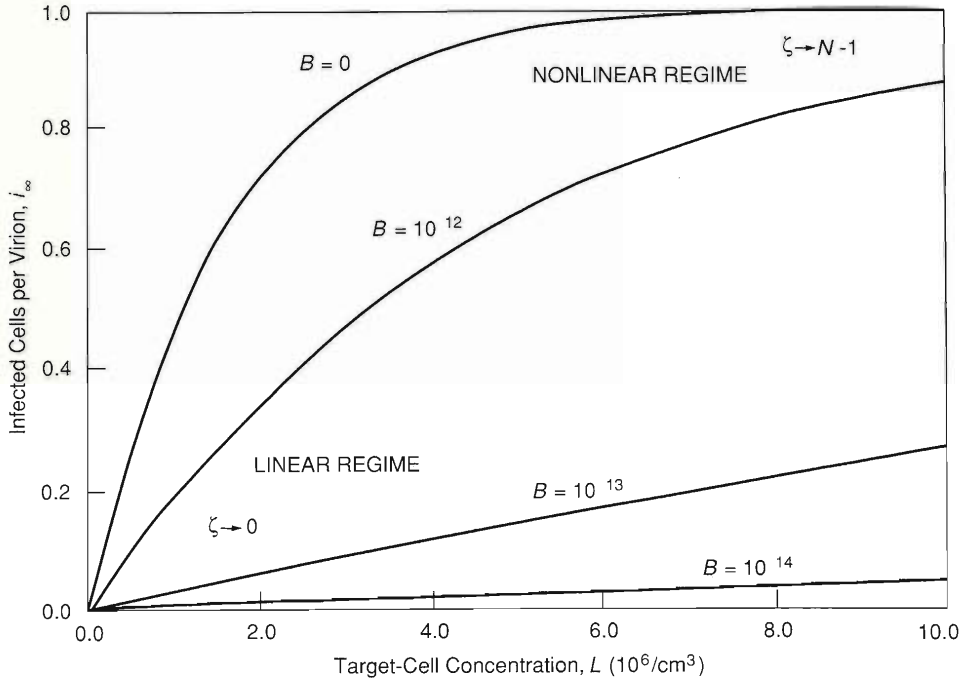

Fig. 6. Numerical solutions of the model illustrate a progression from small to large ζ (see Eqs. 8′ and 9′ in "Mathematical Considerations.") The four solutions correspond to different sCD4 concentrations: $B = 0$, 10^{12}, 10^{13} and 10^{14} molecules cm^{-3}. The life of a virion consists of a race between finding a target cell and inactivation. Small values of ζ reflect a situation in which a virion is likely to have only one chance to infect a target cell in its lifetime. Conversely, large values of ζ reflect a situation in which a virion has multiple chances to infect a target cell. Since we assumed in these calculations that the pre-incubation time, T_p, was 0, small values of ζ occur only when $k_\ell L/[(k_s + k_n)(1 + BK_{assoc})] \ll 1$, that is, when $L \to 0$ or $B \to \infty$. In both instances Eq. 8′ implies that I_∞ is proportional to L. The breakdown of this proportionality occurs as $\zeta \to N - 1$, that is, as $L \to \infty$. The figure also shows the effects of adding various concentrations of sCD4. Notice that the region of transition between linear and nonlinear behavior depends strongly on the blocker concentration. For all solutions $k_n = 0$, $k_s = 10^{-4}$ s^{-1}, and the primary infection time is 18 hours, or 6.48×10^4 seconds.

by Eq. 8′; when $\zeta \to N - 1$ (as it does, for example, when $B \to 0$ and $L \to \infty$) infection is promoted, and I_∞ is approximated by Eq. 9′. Now let's look at numerical results for $i_\infty \equiv I_\infty/V_0$ versus target-cell concentration L at different values of B, the concentration of blocker (Fig. 6). Note that when $\zeta \to 0$, the number of infected cells increases linearly with target-cell concentration. When $\zeta \to N - 1$, the relationship between I_∞ and L is no longer linear. That result is very important for interpreting viral infectivity assays. It says that for some purposes, such as measuring blocker activity, viral infectivity assays are best done at low values of L where I_∞ is proportional to L. The nonlinear relation between I_∞ and L at high L makes comparison of different assays much more difficult.

Determining Rate Constants from Experiment

A primary motivation for developing a kinetic theory is to provide a means for defining and determining meaningful parameters. For the case at hand the main unknown parameters of interest are the rate constants k_ℓ, k_n, k_s, k_f, and k_r. Frequently, we are also ignorant of the exact size of the initial inoculum V_0. Our analysis of the model (see "Mathematical Considerations") indicates that a completely satisfactory solution to the problem of parameter determination is not really possible. For example, it is very difficult to determine the values of the rate constants k_f, and k_r separately. One must thus be satisfied with simply determining the ratio of these quantities $K_{assoc} \equiv k_f/k_r$.

Accurate determinations of K_{assoc} are needed to assess the effectiveness of agents such as sCD4 in blocking infection. To design an experiment to determine K_{assoc}, we

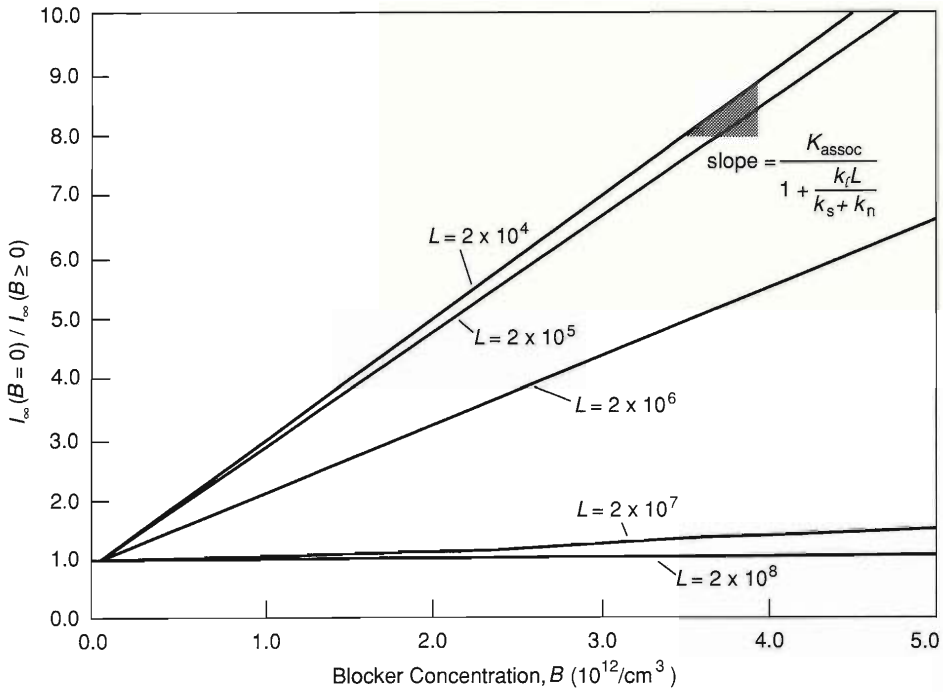

MEASURING BLOCKER AFFINITY

Fig. 7. Numerical solutions simulating a series of infectivity assays for quantifying blocker affinity (K_{assoc}). Affinity is measured by comparing results of an assay without blocker with those of an assay with blocker, holding other conditions constant. This "control"-to-"experiment" ratio is expressed by $I_\infty(B = 0)/I_\infty(B \geq 0)$. The five straight lines correspond to increasing concentrations of target cells: $L = 2 \times 10^4$, 2×10^5, 2×10^6, 2×10^7, and 2×10^8 cells cm^{-3} The slopes corresponding to those concentrations are 2.0×10^{-12}, 1.9×10^{-12}, 1.1×10^{-12}, 8.0×10^{-14}, and 0 cm^3 molecule^{-1}, respectively. According to Eq. 8′, the slopes provide estimates of the quantity $K_{assoc}/[1 + k_\ell L/(k_s + k_n)]$, which is the "apparent" equilibrium constant for the association of blocker and *gp*120. The slope of the curve corresponding to the lowest value of L (the top curve) yields the best estimate of K_{assoc}. For all solutions $T_p = 0$, $k_n = 0$, $k_s = 10^{-4}$ s^{-1}, and I_∞ is the value of I at $T = 6.48 \times 10^4$ seconds.

will use Eq. 8′. In such an experiment I_∞ would be measured at various values of the blocker concentration B, and all other variables would be held constant. For conditions such that $\zeta < 1$, Eq. 8′ implies that a plot of $I_\infty(B = 0)/I_\infty(B \geq 0)$ versus B will be linear with a slope of $K_{assoc}/[1 + k_\ell L/(k_s + k_n)]$ and an intercept of 1. Further, if the experiment is performed within the regime where $k_\ell L(k_s + k_n) \ll 1$, then the slope of such a plot will be a good estimate of K_{assoc}. To simulate such an experiment, we generated numerical solutions to Eqs. 2–5 for various values of B and plotted the appropriate ratio versus B (Fig. 7). Although the plots for all values of L appear linear, only at the lowest target-cell concentrations is the slope a reasonable estimate of K_{assoc}.

A number of publications report that sCD4 blocks HIV infection of CD4$^+$ lymphocytes, but only two provide sufficient information for determining K_{assoc} with the technique shown in Fig. 7. From published data of Deen et al., we determine that $K_{assoc} \approx 3.4 \times 10^{-12}$ cm^3 molecule^{-1}, and from the data of Hussey et al., we calculate that $K_{assoc} \approx 3.8 \times 10^{-12}$ cm^3 molecule^{-1} for two sCD4 derivatives.

Those "biological" results should be compared to the following range of values for K_{assoc} determined by direct "physical" methods: $0.42 \times 10^{-12} \leq K_{assoc} \leq 2.3 \times 10^{-12}$ cm^3 molecule^{-1} for various analogs of sCD4. The close agreement between biological and physical methods strongly supports the fundamental assumption of our model that infection proceeds at a rate proportional to the number of free *gp*120s per virion (equivalent-site approximation). That agreement would not ensue if there were significant infection mechanisms not requiring *gp*120 nor if blocking essentially all *gp*120s was necessary to diminish infection. Since blocking is reversible, it would not ultimately block infection in the absence of nonspecific killing and shed-

MEASURING THE NONSPECIFIC KILLING AND SHEDDING RATE CONSTANTS

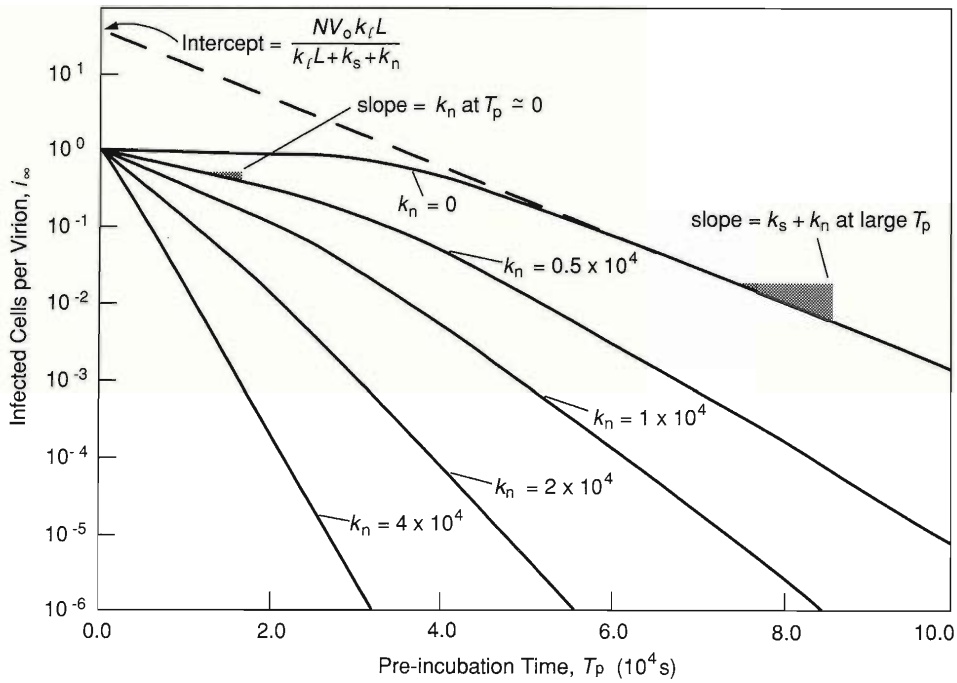

Fig. 8. Five numerical solutions of the model simulating a series of experiments to determine k_s and k_n. In each simulation the virions pre-incubate for various times T_p before being added to a reaction chamber. The five plots correspond to increasing concentrations of nonspecific killing agent: $k_n = 0$, 0.5×10^{-4}, 10^{-4}, 2×10^{-4}, and 4×10^{-4} s^{-1}. The ordinates are normalized by the initial number of virions, a procedure equivalent to taking $V_0 = 1$ in Eqs. 8′ and 9′. Initially the slope of each plot is k_n, but at longer preincubation times the slope increases and approaches $k_s + k_n$. The transition to the final slope occurs when T_p satisfies $\zeta \ll 1$. Equation 7′ implies that extrapolating the final slope to $T_p = 0$ (shown for top curve) gives the intercept $NV_0k_\ell L/(k_\ell L + k_s + k_n)$, which we use to estimate NV_0 and k_ℓ (see Fig. 9). For all solutions $k_s = 10^{-4}$ s^{-1}, $B = 0$, $L = 10^8$ cm^{-3}, and I_∞ is the value of I at $T = 6.48 \times 10^4$ seconds.

ding processes, this is, if k_s and k_n were both zero. The fact that sCD4 is effective verifies that such processes ultimately limit target-cell infection.

A graphic technique similar to that described for estimating K_{assoc} can yield estimates of k_n and $k_s + k_n$ from experimental data. The appropriate experiments would measure I_∞ for various values of T_p, the preincubation time (the time between birth of virions and their addition to an assay chamber). The rate of change of I_∞ with T_p is the decay rate of the infectiousness of the virus. To simulate such experiments we generated numerical solutions of Eqs. 2–5 at five different values of k_n and plotted the resulting curves of I_∞ versus T_p (Fig. 8). Provided the target-cell concentration is as large as possible in vitro ($\approx 10^8$ cells per cm^3 for lymphocytes) and no blocker is added ($B = 0$), Eq. 9′ implies that the slope of each curve at $T_p \approx 0$ is a good estimate of k_n, and Eq. 8′ implies that the slope of each curve at large T_p is a good estimate of $k_s + k_n$. The increase in decay rate with pre-incubation time is a consequence of a fundamental kinetic difference between nonspecific killing and shedding. Nonspecific killing is a so-called single-hit process (it happens all at one time), whereas shedding is a multi-hit process that inactivates the virus via many incremental steps. In other words, the loss of a few *gp*120s makes little difference to the initial infection rate. The quantity $k_s + k_n$ is proportional to the time a viral strain remains infectious. Consequently a change in either k_n or $k_s + k_n$ produced by a viracidal agent provides an objective measure of the potency of that agent.

By conducting two "pre-incubation assays" as described above with different target-cell concentrations, we can estimate both NV_0 and k_ℓ (Fig. 9). Since we have an estimate of N, the quantity NV_0 is useful for estimating V_0, the initial number of infectious virions. The rate constant k_ℓ quantifies the susceptibility of a particular target-cell type to infection by a particular HIV strain. A decrease in k_ℓ can be

caused by a number of independent factors, for example, a decrease in the surface density of CD4 or an increase in the time required for the viral envelope to fuse with the cell membrane and the viral core to enter the cell. A numerical ranking of target-cell tropisms, or affinities, of HIV according to the value of k_ℓ would help to clarify whether reported variations in virulence are due to increased transmission of the virus from cell to cell or to increased replication of the virus within a single cell. The constant k_ℓ is a measure of transmission.

Infection As a Branching Process

In an infectivity assay virions infect target cells (the primary infection phase), then new virions that bud from those infected cells infect other uninfected target cells (secondary infection phase), and so on. Thus an infectivity assay can be likened to a branching process (Fig. 10). Each primary infection generates (on average) V_n secondary virions, which enter the culture medium without pre-incubation ($T_p = 0$). The secondary virions, in turn, infect other target cells with probability i_∞. The infection spreads if the branching number $V_n i_\infty$ (the average number of secondary infections per primary infection) is greater than 1. If $V_n i_\infty \leq 1$, the infection is limited to a small number of cells.

Blocking secondary infections with sCD4 allows estimation of the branching number for unblocked infections. Let's define B_{min} as the minimum sCD4 concentration that extinguishes the branching process. It can be shown that if ζ is not too large (Eq. 8′), then $V_n i_\infty \approx NV_n k_\ell L/(k_s + k_n) \approx (1 + B_{min}K_{assoc})$. Results from Deen et al. suggest that $B_{min} > 10\ \mu g\ cm^{-3} \approx 10^{14}$ molecules cm^{-3}. Using that value for B_{min} and a value for K_{assoc} of 3×10^{-12} cm^3 molecule^{-1} yields a value of $V_n i_\infty$ greater than 300.

That large value may be due to the fact that Deen et al. stimulated the $CD4^+$ lymphocytes in their assay with the mitogen (mitosis-inducing agent) phytohemagglutinin (PHA). Recent work by Gowda et al. suggests that stimulation of human $CD4^+$

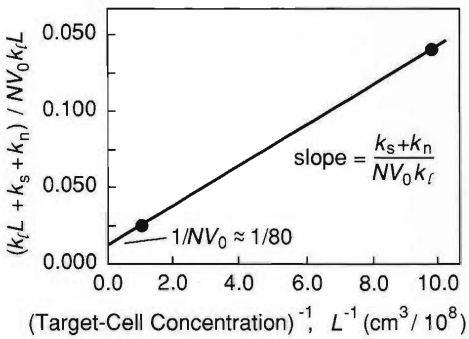

ESTIMATING k_ℓ AND NV_0

Fig. 9. Estimation of NV_0 and k_ℓ by using data from at least two of the "pre-incubation assays" simulated in Fig. 8. Extrapolating the final slope of the top curve of Fig. 8 to $T_p = 0$ gives $NV_0k_\ell L/(k_\ell L + k_s + k_n) \approx 40$, when $L = 10^8$ cm^{-3}. Performing a similar extrapolation when $L = 10^7$ cm^{-3} (with all other conditions identical) gives $NV_0k_\ell L/(k_\ell L + k_s + k_n) \approx 7$ (graph not shown). Plotting the reciprocal of $NV_0k_\ell L/(k_\ell L + k_s + k_n)$ versus $1/L$ gives a straight line with an intercept of $1/NV_0$ and a slope-to-intercept ratio of $(k_s + k_n)/k_\ell$. Since $k_s + k_n$ is given by the final slope in Fig. 7, k_ℓ can be estimated directly.

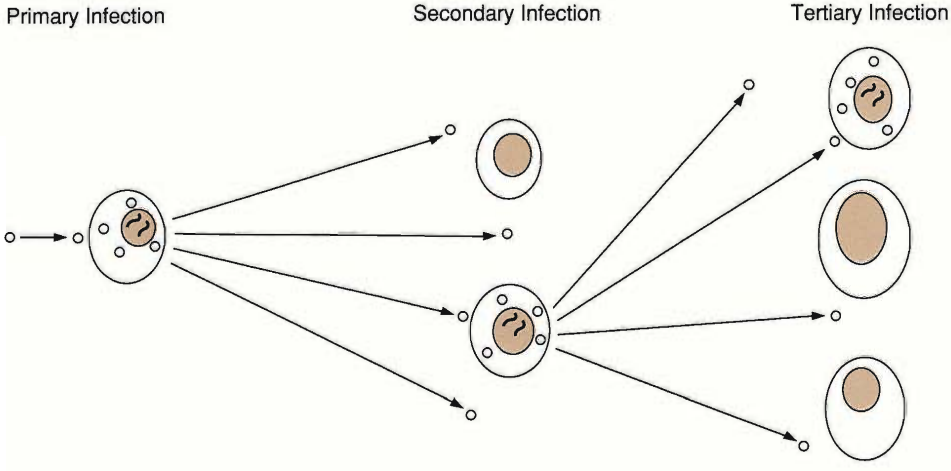

BRANCHING PROCESSES

Fig. 10. The spread of HIV infection from cell to cell by free virions can be viewed as a branching process. Here V_n, the expected number of progeny virions from an infected cell is 4, and i_∞, the probability that a progeny virion will find a target, is 0.25. Since the branching number, or $V_n i_\infty$ is equal to 1, the process is just self-sustaining.

Mathematical Considerations

To facilitate analysis of the rate equations governing the kinetics of a viral infectivity assay (Eqs. 2–5) in the main text), we introduce non-dimensional variables $i \equiv I/V_0$, $v \equiv V/V_0$, $f \equiv F/NV$, $c \equiv C/NV$, and $g \equiv (F+C)/NV = f+c$. We also introduce non-dimensional time $t \equiv (k_s+k_n)T$ and the non-dimensional parameters $\sigma \equiv k_s/(k_s+k_n)$, $\lambda \equiv k_\ell L/(k_s+k_n)$, $\gamma \equiv k_r/(k_s+k_n)$, and $\beta \equiv k_f B/k_r$. Then Eqs. 2–5 become

$$\frac{di}{dt} = N\lambda f v, \tag{1'}$$

$$\frac{dv}{dt} = -(N\lambda f + 1 - \sigma)v, \tag{2'}$$

$$\frac{df}{dt} = -\gamma(\beta f - c) - \sigma f - \lambda f(1-f), \tag{3'}$$

and

$$\frac{dc}{dt} = \gamma(\beta f - c) - \sigma c + \lambda f c. \tag{4'}$$

Because $\gamma \equiv k_r/(k_s+k_n)$ is on the order of 10^4 for physically relevant parameters, perturbation expansions in γ^{-1} of the form $f = f_0 + \gamma^{-1}f_1 + \gamma^{-2}f_2 + \cdots$ and $c = c_0 + \gamma^{-1}c_1 + \gamma^{-2}c_2 + \cdots$ lead to solutions of Eqs. 1′–4′. The zeroth-order truncation, $f = f_0$ and $c = c_0$, is equivalent to the usual quasi-steady-state approximation, $k_f BF \approx k_r C$, which holds for time scales longer than the *gp*120-sCD4 equilibration time. That approximation gives $c \approx \beta g/(1+\beta)$ and $f \approx g/(1+\beta)$.

Adding Eqs. 3′ and 4′ and applying the steady-state approximation yield

$$\frac{dg}{dt} = -\sigma g - \lambda(1+\beta)^{-1} g(1-g), \tag{5'}$$

lymphocytes by mitogens significantly increases the rate at which they are infected by HIV. Therefore, it is conceivable that stimulation with PHA significantly increased the probability of target-cell infection i_∞ and the number of secondary virions V_n. Therefore, additional experiments to determine the branching number of both resting and stimulated lymphocytes are needed.

Since the branching number, $NV_n k_\ell L/(k_s+k_n)$, is proportional to target-cell concentration, we can extrapolate from the conditions of Deen et al. ($L \approx 10^6$ cells cm^{-3} and $B_{min} > 10$ μg cm^{-3}) to the conditions in human blood ($L \approx 10^6$ cells cm^{-3}) and human lymph nodes ($L \approx 10^8$ cells cm^{-3}). Such extrapolation indicates a minimum therapeutic concentration of ≈ 1000 μg cm^{-3} of sCD4 to treat established infections in vivo (a very high concentration). Even more pessimistically, we note that target-cell infection by direct cell-to-cell contact is probably less easily blocked than infection by free virus in the fluid medium. Experiments examining this situation are also required.

The predictions about therapeutic use of sCD4 hold if the only effect of sCD4

which is a form of the Bernoulli equation and can be solved by separation of variables.

Substituting $g(t)$ into Eq. 2′ gives an expression for $v(t)$. Next, substituting $g(t)$ and $v(t)$ into Eq. 1′ gives an expression for $i(t)$. As $t \to \infty$, $i(t)$ can be approximated by

$$i_\infty \approx e^{-(1-\sigma)t_p} \frac{\zeta N}{N-1} e^{-\zeta/\delta} \sum_{j=0}^{\infty} \frac{(\zeta/\delta)^j}{(1+\delta j)j!}, \tag{6′}$$

where $\zeta \equiv [\exp(-\sigma t_p)](N-1)\lambda/(\lambda+1+\beta)$ and $\delta \equiv [\lambda+\sigma(1+\beta)]/(\lambda+1+\beta)$. Equation 6′ is related to the incomplete gamma function, and the approximation that yields it relies on the fact that $N \gg 1$. Notice that $\zeta \leq N-1$ and $\delta \leq 1$.

The parameter ζ is a measure of the degree to which assay conditions promote target cell infection. Expressing ζ in dimensional variables gives

$$\zeta \equiv e^{-(k_s+k_n)T_p} \frac{(N-1)k_\ell L}{k_\ell L + (1+K_{assoc}B)(k_s+k_n)}. \tag{7′}$$

Target-cell infection is less probable as $\zeta \to 0$, that is, as $T_p \to \infty$, $L \to 0$, $B \to \infty$, or $(k_s+k_n) \to \infty$. Conversely, target-cell infection is more probable as $\zeta \to N-1$, that is, as $T_p \to 0$, $L \to \infty$, $B \to 0$, or $(k_s+k_n) \to 0$. Expansions of Eq. 6′ for each of those limits lead to the expressions

$$I_\infty \approx \frac{NV_0 k_\ell L e^{-(k_s+k_n)T_p}}{k_\ell L + (1+BK_{assoc})(k_s+k_n)} \left(1 - \frac{\zeta}{1+\delta} + \cdots\right) \text{ as } \zeta \to 0 \tag{8′}$$

and

$$I_\infty \approx \frac{V_0 N e^{-k_n T_p}}{N-1} \left[1 - \frac{1-\delta}{\zeta} + \cdots\right] \text{ as } \zeta \to N-1. \tag{9′}$$

For both limiting cases δ appears only in the higher-order terms. Note that experimentally I_∞ corresponds to the number of infected cells at $T \approx 10^5$ seconds.

As explained in the main text, Eqs. 7′ and 8′ are useful for the design and analysis of experiments to measure the parameters K_{assoc}, k_s, k_n, k_ℓ, and NV_0. Figure 5 in the main text shows some characteristics of the transition from the regime of Eq. 8′ (small ζ) to the regime of Eq. 9′ (large ζ). ■

is to block free virus from infecting target cells. Siliciano et al. and Lanzavecchia et al. have suggested that sCD4 may also act to protect $CD4^+$ lymphocytes from indirect or autoimmune effects induced by *gp*120. If that is the case, then much lower concentrations of sCD4 may be of therapeutic use.

The branching number can also be used to estimate the immune response that an anti-*gp*120 vaccine must induce to protect against HIV infection. In that instance K_{assoc} is the equilibrium constant for association of *gp*120 and neutralizing antibody (Ig), and B_{min} is the minimum concentration of Ig required to extinguish the spread of infection. Assuming that neutralizing Ig has a K_{assoc} identical to that of sCD4 (a rather high-affinity Ig) and a molecular weight of about 150,000 and that $V_n i_\infty \approx 300$ yields $B_{min} \approx 0.03$ mg cm^{-3} for blood. For lymph nodes we calculate that a concentration of about 3 mg cm^{-3} will be required to prevent growth of infection. Normally, the total concentration of all the hundreds of thousands of antibodies in serum is ≈ 20 mg cm^{-3}. Thus an anti-*gp*120 vaccine must induce and maintain an extremely high concentration of antibody.

Conclusions

Viral infectivity assays have been an indispensable tool for HIV research. However, we believe that their utility can be vastly increased by analyzing the kinetic processes involved rather than treating them like a black box. Analysis of published data using our kinetic model have revealed limitations in present assay designs and ambiguities in assay results. For example, blocker assays (see Fig. 7) are usually not designed to minimize the error in determining K_{assoc} nor to answer more than one question at a time.

Our immediate goal is to increase the quality and amount of information derivable from HIV infectivity assays. We have approached this by defining five parameters—K_{assoc}, k_s, k_n, k_ℓ, and NV_0—characterizing HIV infection of target cells. So far the model has been used successfully to calculate K_{assoc} from a number of published experiments. That success gives us some initial confidence in our model. We will gain additional confidence by calculating the values of the other parameters from experimental data. Then it may be possible to search for processes not included in the model by comparing theory and experiment.

We also plan to expand the model to include intracellular processes (for example, by dividing k_ℓ into components describing viral penetration, uncoating, transcription, maturation, and budding) so that the kinetics of the new class of intracellular blocking agents can be quantified. Finally, our more ambitious goal is to improve the interpretation of infectivity assays in vitro to the point that reliable extrapolations can be made to pathogenic processes in vivo.

Our kinetic model is the first attempt to provide a theoretical foundation for the interpretation of viral infectivity assays. We hope that our presentation makes clear the practical value of a rigorous mathematical approach to the problem. ■

Further Reading

Keith C. Deen, J. Steven McDougal, Richard Inacker, Gail Folena-Wasserman, Jim Arthos, Jonathan Rosenberg, Paul Jay Maddon, Richard Axel, and Raymond W. Sweet. 1988. A soluble form of CD4 (T4) protein inhibits AIDS virus infection. *Nature* 331:82–84.

Shantharaj D. Gowda, Barry S. Stein, Nahid Mohagheghpour, Claudia J. Benike, and Edgar G. Engleman. 1989. Evidence that T cell activation is required for HIV-1 entry in $CD4^+$ lymphocytes. *Journal of Immunology* 142:773–780.

Robert F. Siliciano, Trebor Lawton, Cindy Knall, Robert W. Karr, Phillip Berman, Timothy Gregory, and Ellis L. Reinherz. 1988. Analysis of host-virus interactions in AIDS with anti-gp120 T cell clones: Effect of HIV sequence variation and a mechanism for $CD4^+$ cell depletion. *Cell* 54:561–575.

Antonio Lanzavecchia, Eddy Roosnek, Tim Gregory, Phillip Berman, and Sergio Abrignani. 1988. T cells can present antigens such as HIV gp120 targeted to their own surface molecules. *Nature* 334:530–532.

Rebecca E. Hussey, Nneil E. Richardson, Mark Kowalski, Nicholas R. Brown, Hsiu-Ching Chang, Robert F. Siliciano, Tatyana Dorfman, Bruce Walker, Joseph Sodroski, and Eellis L. Reinherz. 1988. A soluble CD4 protein selectively inhibits HIV replication and syncytium formation. *Nature* 331:78–81.

Cecilia Cheng-Mayer, Deborah Seto, Masatoshi Tateno, and Jay A. Levy. 1988. Biologic features of HIV-1 that correlate with virulence in the host. *Science* 240:80–82.

Anthony S. Fauci. 1988. The human immunodeficiency virus: infectivity and mechanisms of pathogenesis. *Science* 239:617–622.

Amanda G. Fisher, Barbara Ensoli, David Looney, Amdrea Rose, Robert C. Gallo, Michael S. Saag, George M. Shaw, Beatrice H. Hahn, and Flossie Wong-Staal. 1988. Biologically diverse molecular variants within a single HIV-1 isolate. *Nature* 334:444–447.

Scott P. Layne, John L. Spouge and Micah Dembo. 1989. Quantifying the infectivity of HIV. Proceedings of the *National Academy of Sciences of the United States of America*, in press.

Laurence A. Lasky, Gerald Nakamura, Douglas H. Smith, Christopher Fennie, Craig Shimasaki, Eric Patzer, Phillip Berman, Timothy Gregory, and Daniel J. Capon. 1987. Delineation of a region of the human immunodeficiency virus type 1 gp120 glycoprotein critical for interaction with the CD4 receptor. *Cell* 50:975–985.

Peter L. Nara, W. C. Hatch, N. M. Dunlop, W. G. Robey, L. O. Arthur, M. A. Gonda and P. J. Fischinger. 1987. Simple, rapid, quantitative, syncytium-forming microassay for the detection of human immunodeficiency virus neutralizing antibody. *AIDS Research and Human Retroviruses* 3:283–302.

M. Özel, G. Pauli, and H. R. Gelderblom. 1988. The organization of the envelope projections on the surface of HIV. *Archives of Virology* 100:255–266.

Douglas H. Smith, Randal A. Byrn, Scot A. Marsters, Timothy Gregory, Jerome E. Groopman, and Daniel J. Capon. 1987. Blocking of HIV-1 infectivity by a soluble, secreted form of the CD4 antigen. *Science* 238:1704–1707.

John L. Spouge, Scott P. Layne and Micah Dembo. 1989. Analytic results for quantifying HIV infectivity. *Bulletin of Mathematical Biology*, in press.

Micah Dembo earned his B.S. in mathematics from Allegheny College in 1972 and his Ph.D. in biomathematics from Cornell University Medical College in 1977. After finishing graduate work he came to Los Alamos as a postdoctoral fellow in the Theoretical Biology and Biophysics Group and remained as a staff member after the appointment ended. During his years in the group, he has worked on a number of theoretical problems of importance in biology. In addition to developing mathematical models of cell activation and desensitization, he has worked on the modeling of cooperative interactions in proteins, on diffusion reaction problems, particularly with regard to membrane transport phenomena, and on fluid mechanical models of cell motility. In 1982 the National Institutes of Health awarded him a Research Career Development Award to work in cell motility.

Scott P. Layne is a Long Term Visiting Staff Member in the Mathematical Modeling Group of the Theoretical Division at Los Alamos and a staff member at Lawrence Livermore National Laboratory. He studied chemistry at Depauw University and attended medical school at Case Western Reserve University. After finishing an internship he was a postdoctoral fellow at the Center for Nonlinear Studies at Los Alamos, where he looked for evidence of nonlinear excitations (solitons) in living cells. Scott has also studied at Stanford University's Department of Applied Physics. In addition to AIDS epidemiology, he works on quantifying the infectivity of HIV.

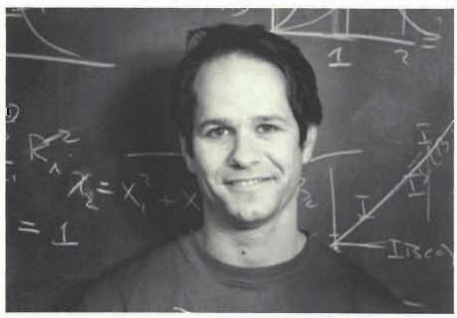

John L. Spouge was born in Sheffield, England, and educated at the University of British Columbia, where he earned his B.S. and M.D. degrees and Oxford University where he earned a Ph.D. in mathematics. He was a postdoctoral fellow at Los Alamos from 1983 to 1985. Currently, he is employed at the National Institutes of Health in Bethesda, Maryland. His research interests include developing systematic statistical methods of evaluating and organizing sequence information (such as that found in DNA), examining the physics of diffusion-controlled reactions, and developing more efficient algorithms for sequence alignments with a view to developing programs that do mutiple-sequence alignments and structure predictions. This latter work has yielded a general theory for improving sequence-alignment algorithms as well as code that is demonstrably faster for two sequences and that may prove dramatically faster for multiple sequences.